JCI The Journal of Clinical Investigation

Functional characterization of CD4+ T cell receptors crossreactive for SARS-CoV-2 and endemic coronaviruses

Arbor G. Dykema, … , Joel N. Blankson, Kellie N. Smith

J Clin Invest. 2021;131(10):e146922. https://doi.org/10.1172/JCI146922.

Clinical Medicine COVID-19 Immunology

Graphical abstract

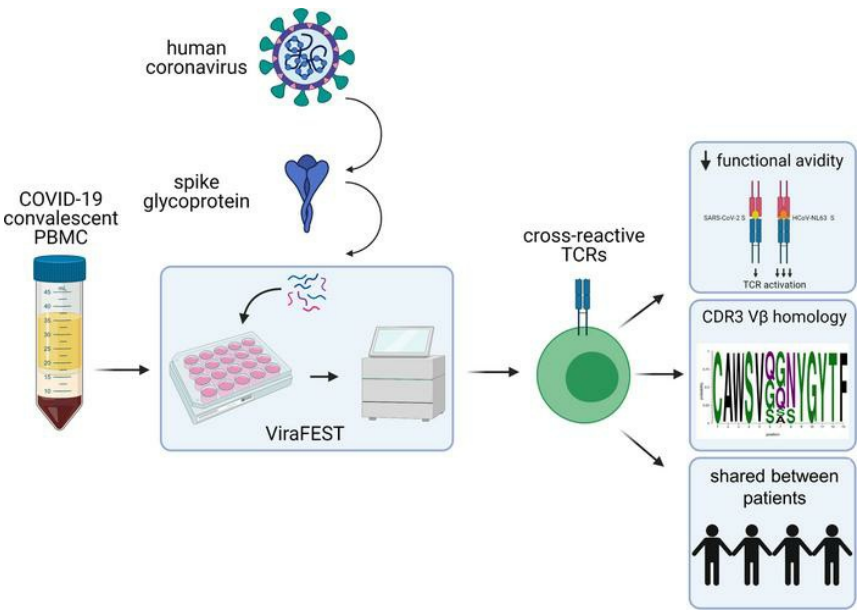

Functional characterization of CD4+ T cell receptors crossreactive for SARS-CoV-2 and endemic coronaviruses

Arbor G. Dykema,[1,2] Boyang Zhang,[3] Bezawit A. Woldemeskel,[4] Caroline C. Garliss,[4] Laurene S. Cheung,[1,2] Dilshad Choudhury,[1,2] Jiajia Zhang,[1,2] Luis Aparicio,[1,2] Sadhana Bom,[1,2] Rufiaat Rashid,[1,2] Justina X. Caushi,[1,2] Emily Han-Chung Hsiue,[2,5,6,7] Katherine Cascino,[4] Elizabeth A. Thompson,[1,2] Abena K. Kwaa,[4] Dipika Singh,[1,2] Sampriti Thapa,[1,2] Alvaro A. Ordonez,[8] Andrew Pekosz,[9] Franco R. D'Alessio,[4] Jonathan D. Powell,[1,2] Srinivasan Yegnasubramanian,[2] Shibin Zhou,[2,5,6,7] Drew M. Pardoll,[1,2] Hongkai Ji,[3] Andrea L. Cox,[1,4] Joel N. Blankson,[4] and Kellie N. Smith[1,2]

[1]Bloomberg~Kimmel Institute for Cancer Immunotherapy, [2]Sidney Kimmel Comprehensive Cancer Center, [3]Department of Biostatistics, School of Public Health, [4]Department of Medicine, School of Medicine, and [5]Ludwig Center, Sidney Kimmel Comprehensive Cancer Center, Johns Hopkins University, Baltimore, Maryland, USA. [6]Howard Hughes Medical Institute, Chevy Chase, Maryland, USA. [7]Lustgarten Pancreatic Cancer Research Laboratory, Sidney Kimmel Comprehensive Cancer Center, [8]Department of Pediatrics, School of Medicine, and [9]Department of Molecular Microbiology and Immunology, School of Public Health, Johns Hopkins University, Baltimore, Maryland, USA.

BACKGROUND. Recent studies have reported T cell immunity to the severe acute respiratory syndrome coronavirus 2 (SARS-CoV-2) in unexposed donors, possibly due to crossrecognition by T cells specific for common cold coronaviruses (CCCs). True T cell crossreactivity, defined as the recognition by a single TCR of more than one distinct peptide-MHC ligand, has never been shown in the context of SARS-CoV-2.

METHODS. We used the viral functional expansion of specific T cells (ViraFEST) platform to identify T cell responses crossreactive for the spike (S) glycoproteins of SARS-CoV-2 and CCCs at the T cell receptor (TCR) clonotype level in convalescent COVID-19 patients (CCPs) and SARS-CoV-2–unexposed donors. Confirmation of SARS-CoV-2/CCC crossreactivity and assessments of functional avidity were performed using a TCR cloning and transfection system.

RESULTS. Memory CD4+ T cell clonotypes that crossrecognized the S proteins of SARS-CoV-2 and at least one other CCC were detected in 65% of CCPs and unexposed donors. Several of these TCRs were shared among multiple donors. Crossreactive T cells demonstrated significantly impaired SARS-CoV-2–specific proliferation in vitro relative to monospecific CD4+ T cells, which was consistent with lower functional avidity of their TCRs for SARS-CoV-2 relative to CCC.

CONCLUSIONS. Our data confirm, for what we believe is the first time, the existence of unique memory CD4+ T cell clonotypes crossrecognizing SARS-CoV-2 and CCCs. The lower avidity of crossreactive TCRs for SARS-CoV-2 may be the result of antigenic imprinting, such that preexisting CCC-specific memory T cells have reduced expansive capacity upon SARS-CoV-2 infection. Further studies are needed to determine how these crossreactive T cell responses affect clinical outcomes in COVID-19 patients.

FUNDING. NIH funding (U54CA260492, P30CA006973, P41EB028239, R01AI153349, R01AI145435-A1, R21AI149760, and U19A1088791) was provided by the National Institute of Allergy and Infectious Diseases, the National Cancer Institute, and the National Institute of Biomedical Imaging and Bioengineering. The Bloomberg~Kimmel Institute for Cancer Immunotherapy, The Johns Hopkins University Provost, and The Bill and Melinda Gates Foundation provided funding for this study.

Authorship note: AGD and BZ contributed equally to this work.

Conflict of interest: DMP and KNS have filed for patent protection on a subset of the technologies described herein (MANAFEST – A Novel Sensitive, Specific, Salable and Simple Method to Identify Functional Anti-Tumor T Cell Responses, US provisional patent application no. 62/407,820). AGD, ALC, FRD, DMP, JNB, and KNS have filed for patent protection on a subset of the technologies described herein (SARS-CoV-2-specific T cell receptors and Related Materials and Methods of Use, US provisional patent application no. 63/135,534). SZ is a founder of, holds equity in, and serves as a consultant to Personal Genome Diagnostics. SZ holds equity in Thrive Earlier Detection and has a research agreement with BioMed Valley Discoveries Inc. DMP reports stock and ownership interests in Aduro Biotech, DNAtrix, Dracen Pharmaceuticals, Dragonfly Therapeutics, Ervaxx, Five Prime Therapeutics, Potenza Therapeutics, RAPT, Tizona Therapeutics, Trieza Therapeutics, and WindMIL; a consulting or advisory role in Amgen, DNAtrix, Dragonfly Therapeutics, Ervaxx, Five Prime Therapeutics, Immunocore, Immunomic Therapeutics, Janssen Pharmaceuticals, MedImmune/AstraZeneca, Merck, RAPT, and WindMIL; research grants from Compugen; patent royalties, and/or other intellectual property through their institution with Aduro Biotech, Arbor Pharmaceuticals, Bristol-Myers Squibb, Immunomic Therapeutics, NexImmune, and WindMIL; and travel, accommodations, and expenses from Bristol-Myers Squibb and Five Prime Therapeutics. KNS receives commercial research funding from Bristol-Myers Squibb, AstraZeneca, and Enara Bio and has received travel support/honoraria from Illumina Inc. KNS, DMP, and SZ own founder's equity in ManaT Bio. These arrangements have been reviewed and approved by the Johns Hopkins University in accordance with its conflict-of-interest policies.

Submitted: December 15, 2020; **Accepted:** April 7, 2021; **Published**: April 8, 2021.

Reference information: J Clin Invest. 2021;131(10):e146922. https://doi.org/10.1172/JCI146922.

Introduction

The 2019 SARS-CoV-2 outbreak and ensuing global pandemic have resulted in significant global morbidity and mortality. Coronavirus disease 19 (COVID-19) symptom severity ranges from mild, or even asymptomatic, to the development of acute respiratory distress syndrome (ARDS), hospitalization, and death (1, 2). It is not unusual for viral illnesses to induce a range of symptom severity, and preexisting immunity to similar but not identical pathogens is generally thought to mitigate disease severity upon reinfection (3–5). Indeed, Sagar et al., suggested that patients with recent infection by 1 of the 4 known endemic human common cold coronaviruses (CCCs) (HCoV-NL63, HCoV-OC43, HCoV-229E, and HCoV-HKU1; ref. 6) experienced less severe COVID-19 illness (7). However, given that 7.5% of people are documented to be infected with a CCC during a given respiratory virus season and that repeated infection with CCCs is common (8–10), it is unlikely that prior CCC exposure alone results in effective viral clearance with minimal disease severity.

One contributing factor to the spectrum of disease severity between patients could be a difference in the development and/or function of severe acute respiratory syndrome coronavirus 2–specific (SARS-CoV-2–specific) T cell–mediated immunity. Ultimately, because B cell responses to antigen (class switching, affinity maturation, and memory) are $CD4^+$ T helper dependent, the quality and durability of humoral responses to SARS-CoV-2 are intimately linked to the $CD4^+$ T cell response. $CD4^+$ T cell responses are readily detected in the majority of recovered COVID-19 patients (11–13), and SARS-CoV-2–specific T cell responses have been detected in SARS-CoV-2–unexposed donors (14–20). Thus, preexisting T cell immunity to CCC could affect SARS-CoV-2 immunity and clinical outcomes in COVID-19 patients. True T cell crossreactivity is defined as the reaction of T cells to more than one distinct peptide-MHC ligand and is mediated by a single T cell clonotype expressing a unique T cell receptor (TCR) heterodimer. A crossreactive T cell response can be due to a number of things: (a) plasticity of complementarity determining region 3 (CDR3) loop regions, (b) promiscuous TCR/MHC binding, and (c) flexibility of the peptide/MHC interaction (21). However, a likely cause of a crossreactive T cell response is peptide homology in certain residues that are required for MHC and TCR binding and recognition. In the case of the coronavirus family, there are a multitude of shared epitopes between SARS-CoV-2 and other coronaviruses, including those that are endemic to the human population (22). Recognition of one of these shared epitopes may allow for a single T cell to crossrecognize both SARS-CoV-2 and CCCs. The precise nature of the SARS-CoV-2/CCC crossreactive response, including whether it is mediated by one or several T cell clonotypes recognizing antigens from different viruses, has not been determined.

In the present study we leverage the viral functional expansion of specific T cells (ViraFEST) assay (23–26), which identifies TCRs corresponding to memory antigen-specific T cells, to evaluate memory $CD4^+$ T cell CCC/SARS-CoV-2 crossreactivity at the clonal level in cells obtained before (n = 7) or during (n = 12) the COVID-19 pandemic. We identified and characterized the TCR clonality and functional avidity of memory T cells crossreactive for the spike glycoprotein (S) of both SARS-CoV-2 and one or more CCCs. We found crossreactive clones that were shared among several of our convalescent COVID-19 patients (CCPs) and unexposed, i.e., pre-COVID (PC) donors and were of lower functional avidity than noncrossreactive clones, together supporting the phenomenon of antigenic imprinting by previous exposure to CCC. The findings presented here underscore the importance of antigen-specificity studies of SARS-CoV-2 to facilitate our understanding of the mechanisms underpinning effective immunity to this virus.

Results

$CD4^+$ T cells from COVID-19 convalescent patients are crossreactive for SARS-CoV-2 and CCC spike proteins. Our central hypothesis is that unique, individual $CD4^+$ T cell clonotypes recognize epitopes from both CCC and SARS-CoV-2 S proteins. This is supported by prior studies demonstrating that some donors have T cell reactivity to the SARS-CoV-2 S antigen without ever being exposed to the virus (12–14, 16, 17). Bona fide crossreactivity mediated by a single T cell clonotype expressing a unique TCR heterodimer has not yet been shown for T cells that target SARS-CoV-2. To address the hypothesis that the same $CD4^+$ T cell clonotypes recognize both SARS-CoV-2 and CCC S peptides, we used the ViraFEST assay to detect S protein–specific T cell clones in the peripheral blood of CCPs and PCs (Figure 1 and Supplemental Table 1; supplemental material available online with this article; https://doi.org/10.1172/JCI146922DS1). The ViraFEST assay identifies canonical antigen-specific memory T cell responses and the cognate TCR(s) contributing to this response via a 10-day T cell culture with relevant antigen followed by TCR Vβ CDR3 sequencing (23–25, 27, 28). This assay has been successfully used to identify TCRs specific for tumor and viral antigens (25, 27) and, more importantly, TCRs crossreactive for related viral epitope variants (26). Using this assay, we tested peripheral blood $CD4^+$ T cells from each donor (Figure 1 and Supplemental Table 1) for reactivity to pooled peptides making up the entirety of the S protein from SARS-CoV-2 and 4 known CCCs, HCoV-NL63, HCoV-OC43, HCoV-229E, and HCoV-HKU1, as cell number allowed. Functional $CD4^+$ T cell clonal expansion was measured from each peptide condition in biological replicate wells using quantitative TCR CDR3 Vβ sequencing. Our stringent data-driven statistical algorithm (23) enabled us to identify antigen-specific $CD4^+$ TCR clonotype expansions in response to one or more S proteins. True crossreactivity was defined by the same $CD4^+$ TCR clonotype seen functionally expanding in response to SARS-CoV-2 S and at least one other CCC S protein.

Consistent with other studies, we detected SARS-CoV-2–specific memory $CD4^+$ T cell responses in 100% of the CCPs tested (n = 12; Supplemental Figure 1, A–L). Strikingly, 8 of these patients (67%) also had TCRs crossreactive for the S protein from SARS-CoV-2 and at least one other CCC, as evidenced by clonal expansion of the same TCR Vβ CDR3 clonotype in response to multiple S protein peptide pools (Figure 2, A–H). While responses were also detected against the SARS-CoV-2 nucleocapsid (N) protein and the CMV, EBV, and flu (CEF) control, as expected, none of these TCRs were crossreactive with any of the S proteins, indicating that crossreactivity relies on protein homology. Crossreactivity to the S protein of 2 or more CCCs occurred in all CCP donors in which we tested multiple CCC S peptide pools (Supplemental Fig-

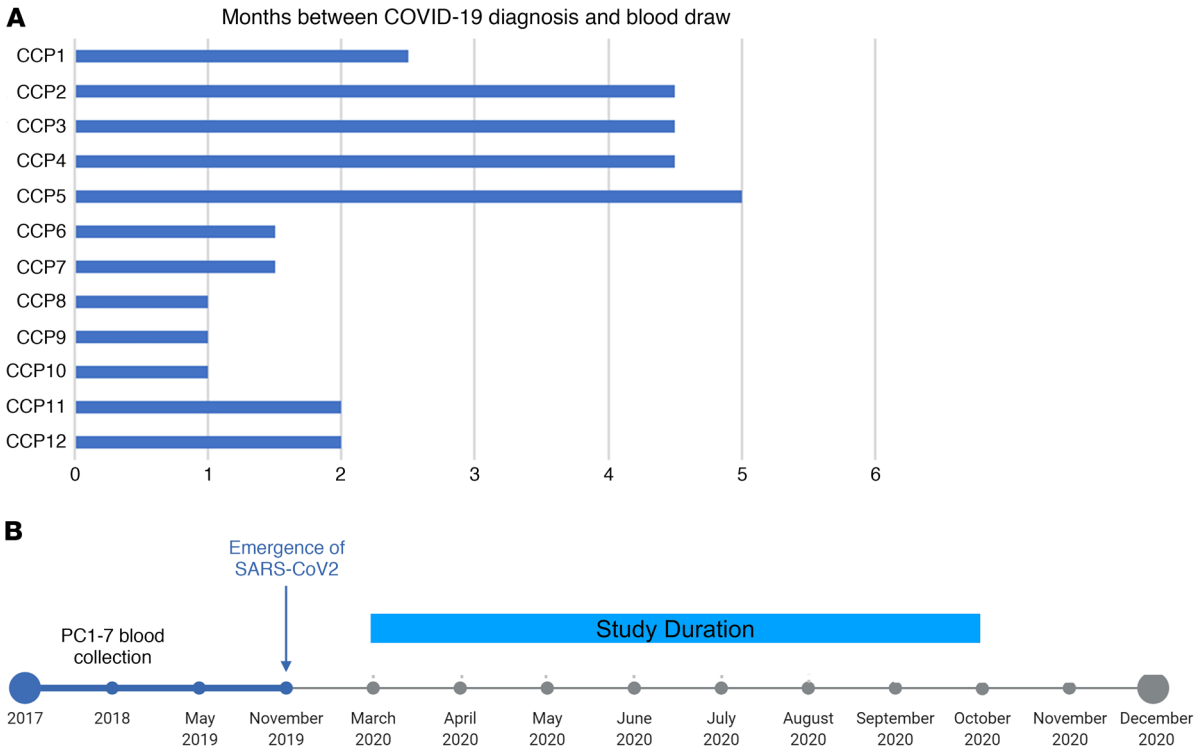

Figure 1. COVID-19 diagnosis to blood draw time line. The number of months from COVID-19 diagnosis to blood sample (*x* axis) matched to COVID-19 convalescent patient on *y* axis (**A**). The study time line indicates the time frame of PC blood collection prior to SARS-CoV-2 emergence and the duration of our study time line from the first COVID-19 diagnosis to the last blood collection date (**B**).

ure 3, A–J). Surprisingly, SARS-CoV-2/HCoV-NL63 crossreactive memory responses by 3 highly homologous TCR-β CDR3 clonotypes (CAWSVQQNYGYTF, CAWSVGGNYGYTF, and CAWSVQGNYGYTF) were independently detected in more than one CCP (red clones; Figure 2, B–D). TCR sequencing of baseline and CEF-stimulated naive and memory $CD4^+$ T cells confirmed that the ViraFEST assay detects memory T cell responses rather than primary responses induced during the 10-day culture (Supplemental Figure 4), as even in the few cases where antigen-specific clones are detected in the naive population, these expansions did not replicate and therefore would not have passed our stringent criteria for identifying antigen-specific responses.

To determine whether $CD4^+$ crossreactive clonotypic expansions were also associated with a crossreactive cytokine profile, $CD4^+$ T cells from CCP6 and CCP12 were cultured separately with SARS-CoV-2 S, HCoV-NL63 S, or without peptide and were each rechallenged with SARS-CoV-2 S, HCoV-NL63 S, or without peptide, followed by intracellular cytokine staining. Consistent with our ViraFEST results, CCP6 demonstrated crossreactive production of IL-2 and IFN-γ, while CCP12 only had monoreactive responses (Supplemental Figure 5). Together, these data show that SARS-CoV-2/CCC crossreactive memory $CD4^+$ T cells are readily detected in the peripheral blood of CCPs and can functionally expand upon antigenic stimulation and that a subset of TCR Vβ CDR3 clonotypes is shared among patients.

SARS-CoV-2–specific TCR avidity and epitope identification. A recent study demonstrated reduced avidity of the SARS-CoV-2/CCC crossreactive T cell response (29); however, this has not been evaluated at the individual clonotype level. To determine the avidity of individual SARS-CoV-2 reactive TCRs, we identified the cognate α chain for 8 monoreactive (recognizing only SARS-CoV-2 S) and 5 crossreactive TCRs detected in CCP4 using the ViraFEST assay (Figure 2B and Supplemental Figure 1D), including the 3 TCRs that were detected in multiple patients. We then cloned the entire TCR gene block into a CD4-overexpressing Jurkat NFAT-luciferase reporter system, which specifically reads out the quantitative strength of TCR engagement via NFAT activation, commonly referred to as functional avidity. Monoreactivity for SARS-CoV-2 S was validated for all 8 TCRs tested (Figure 3, A–H). To map the precise SARS-CoV-2 and HCoV-NL63 S protein region(s) eliciting these responses, we tested 3 monoreactive and all 5 crossreactive TCRs for reactivity against minipools of 10 peptides each to span the entirety of the S protein. TCR-transfected Jurkat reporter cells were stimulated with each pool (Supplemental Figure 6, A and B) and subsequently with individual 15 mer peptides from the positive pools (SARS-CoV-2 pool 12 and HCoV-NL63 pool 15; Supplemental Table 3). Of the 3 monoreactive TCRs (Figure 4A), 2 recognized SARS-CoV-2 (GINITRFQTLLALHRSY, residues 232–248) and 1 recognized SARS-CoV-2 (QFCNDPFLGVYHKNNK, residues 134–150) (Figure 4B and Supplemental Figure 6, D and E), which are both present in the S1 N-terminal domain (30) (Supplemental Figure 7). The EC_{50} for these TCRs ranged from 0.37 μg/ml to 0.77 μg/ml, with an average of 0.6 μg/ml. (Figure 4B).

Crossreactivity was also confirmed for all 5 TCRs tested (Figure 4C), with lower NFAT activity induced by SARS-CoV-2 relative to HCoV-NL63 S protein. All crossreactive TCRs recognized

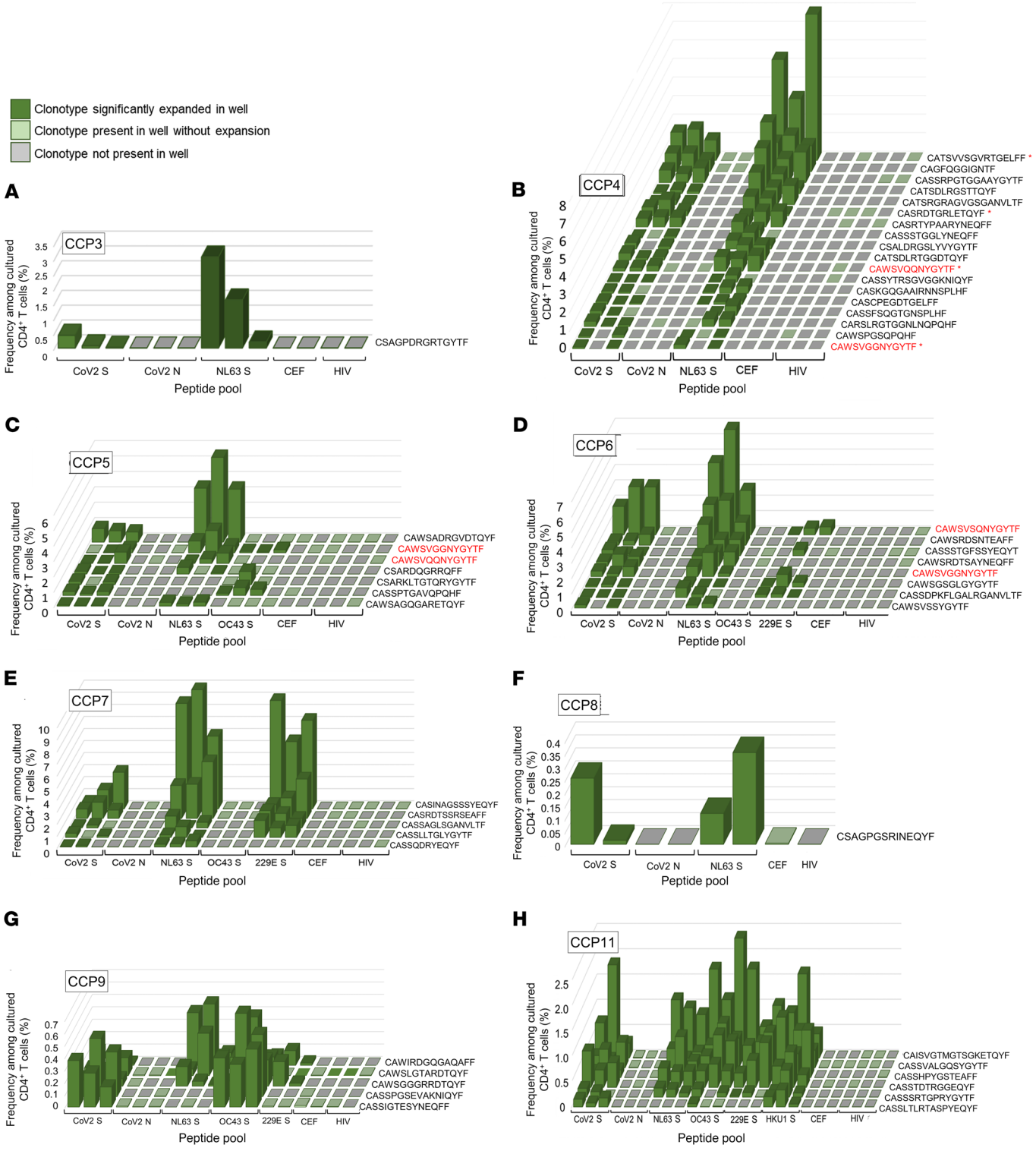

Figure 2. Detection of memory CD4⁺ T cell clonotypes that crossrecognize SARS-CoV-2 and CCC spike proteins. The ViraFEST assay detected crossreactivity to the S protein from SARS-CoV-2 and at least 1 other CCC (HCoV-NL63, HCoV-OC43, HCoV-229E, and HCoV-HKU1) in 8 out of 12 CCPs tested (**A**–**H**). Peptide coculture was done in triplicate unless otherwise noted. Data are shown as the frequency (%) after culture (*y* axis) of antigen-specific CD4⁺ T cell clonotypes (*z* axis) for all peptide pools tested (*x* axis). The top 5 monoreactive TCR Vβ CDR3 amino acid clonotypes for each CCP are shown. Solid green bars represent significant (FDR < 0.05) clonotypic expansion in response to the indicated antigenic peptide pool(s), whereas translucent green color indicates the clonotype was present at low frequency in the well, but did not significantly expand. Gray indicates the relevant TCR clonotype was not detected in that well. An identical, shared TCR Vβ CDR3 amino acid clonotype corresponding to crossreactive memory CD4⁺ T cells in CCP4, CCP5, and CCP6 is shown in red (**B**–**D**). Single-cell TCR sequencing was performed on stimulated CD4⁺ T cells from CCP4 to identify the cognate TCR α chain for TCR β chains of interest (asterisks).

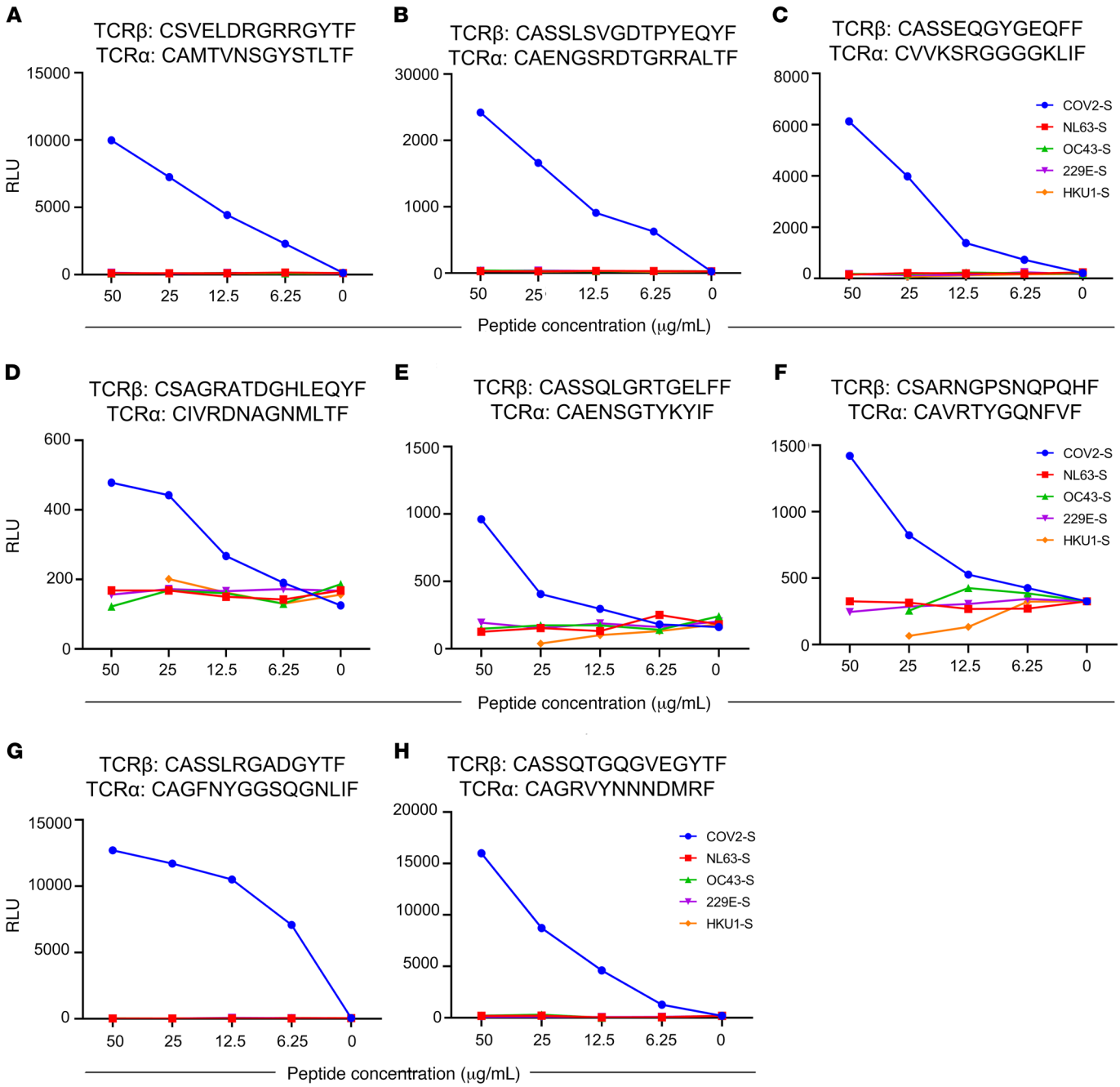

Figure 3. Confirmation of SARS-CoV-2 monoreactivity. (**A**–**H**) SARS-CoV-2 monoreactive TCRs as determined by ViraFEST were cloned and transfected into Jurkat reporter cell line. Jurkats expressing the TCRs of interest were cocultured at a 1:1 ratio with CCP4 LCL and SARS-CoV-2 or all CCC S protein peptide pools in titrating concentrations or without peptide. Data are shown as RLUs at each pool concentration. These data are representative of all experiments repeated twice.

SARS-CoV-2 (SKRSFIEDLLFNKVTLA, amino acids 813–829), which is in the S2 linker region (30) (Supplemental Figure 7) and crossrecognized the IAGRSALEDLLFSKVVT (residues 867–883) region from HCoV-NL63 S (Figure 4D, Supplemental Figure 6C, and Supplemental Table 3). Both of these regions have recently been shown to be crossrecognized by antibodies of CCPs (31). The SARS-CoV-2 sequence, EDLLFNKV, within this 17 mer could represent the core 8 mer responsible for TCR contact and/or MHC class II binding regions and differs from the cognate HCoV-NL63 sequence by only one amino acid substitution, an asparagine to serine at position 6 (EDLLFSKV), which likely does not alter the polarity of the peptide. Peptide titration experiments defined a maximum relative luminescence unit (RLU) range of 4360 to 27,900 for HCoV-NL63 (IAGRSALEDLLFSKVVT) (Figure 4D). The maximum RLU for SARS-CoV-2 (SKRSFIEDLLFNKVTLA) was not reached at 20 μg/ml, but ranged from 2890 to 18,300. The crossreactive TCR functional avidity (EC_{50}, peptide concentration required to reach one-half maxi-

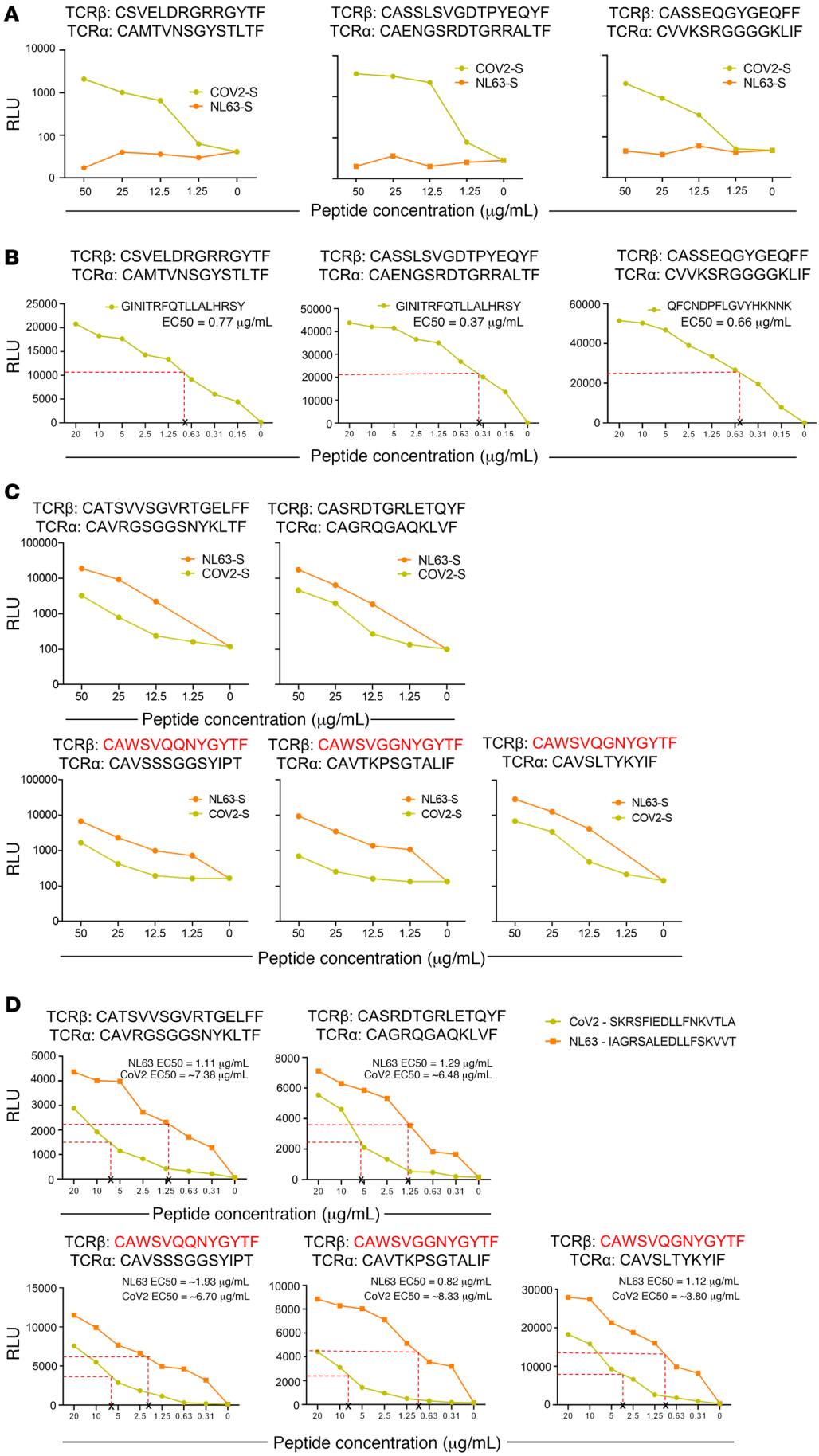
A
TCRβ: CSVELDRGRRGYTF
TCRα: CAMTVNSGYSTLTF
TCRβ: CASSLSVGDTPYEQYF
TCRα: CAENGSRDTGRRALTF
TCRβ: CASSEQGYGEQFF
TCRα: CVVKSRGGGGKLIF
RLU
COV2-S
NL63-S
Peptide concentration (μg/mL)
B
TCRβ: CSVELDRGRRGYTF
TCRα: CAMTVNSGYSTLTF
GINITRFQTLLALHRSY
EC50 = 0.77 μg/mL
TCRβ: CASSLSVGDTPYEQYF
TCRα: CAENGSRDTGRRALTF
GINITRFQTLLALHRSY
EC50 = 0.37 μg/mL
TCRβ: CASSEQGYGEQFF
TCRα: CVVKSRGGGGKLIF
QFCNDPFLGVYHKNNK
EC50 = 0.66 μg/mL
C
TCRβ: CATSVVSGVRTGELFF
TCRα: CAVRGSGGSNYKLTF
TCRβ: CASRDTGRLETQYF
TCRα: CAGRQGAQKLVF
TCRβ: CAWSVQQNYGYTF
TCRα: CAVSSSGGSYIPT
TCRβ: CAWSVGGNYGYTF
TCRα: CAVTKPSGTALIF
TCRβ: CAWSVQGNYGYTF
TCRα: CAVSLTYKYIF
D
TCRβ: CATSVVSGVRTGELFF
TCRα: CAVRGSGGSNYKLTF
NL63 EC50 = 1.11 μg/mL
CoV2 EC50 = ~7.38 μg/mL
TCRβ: CASRDTGRLETQYF
TCRα: CAGRQGAQKLVF
NL63 EC50 = 1.29 μg/mL
CoV2 EC50 = ~6.48 μg/mL
CoV2 - SKRSFIEDLLFNKVTLA
NL63 - IAGRSALEDLLFSKVVT
TCRβ: CAWSVQQNYGYTF
TCRα: CAVSSSGGSYIPT
NL63 EC50 = ~1.93 μg/mL
CoV2 EC50 = ~6.70 μg/mL
TCRβ: CAWSVGGNYGYTF
TCRα: CAVTKPSGTALIF
NL63 EC50 = 0.82 μg/mL
CoV2 EC50 = ~8.33 μg/mL
TCRβ: CAWSVQGNYGYTF
TCRα: CAVSLTYKYIF
NL63 EC50 = 1.12 μg/mL
CoV2 EC50 = ~3.80 μg/mL
RLU
Peptide concentration (μg/mL)

Figure 4. Functional validation and avidity of SARS-CoV-2– and HCoV-NL63 S–reactive TCRs. Single-cell TCR sequencing was performed to identify the cognate TCR-α of SARS-CoV-2 monoreactive (**A** and **B**) and SARS-CoV-2/HCoV-NL63 crossreactive (**C** and **D**) and TCR-β clonotypes. TCRs were cloned and transfected into a Jurkat NFAT-luciferase reporter cell line. Jurkat cells expressing TCRs of interest were cocultured at 1:1 ratio with patient LCL and SARS-CoV-2 S or HCoV-NL63 S peptide pools in titrating concentrations of S protein peptide pools (**A** and **C**) or the mapped 17 mer (**B** and **D**). Data are shown as RLUs at each pool or peptide concentration. Functional avidity for the specific 17 mer epitope was determined by calculating an EC_{50} (concentration at which response was one-half of maximum RLU, black x). These data are representative of all experiments repeated twice.

mum RLU) for HCoV-NL63 S (IAGRSALEDLLFSKVVT) ranged from 0.82 μg/ml to 1.93 μg/ml, with a mean of 1.25 μg/ml. The SARS-CoV-2 S (SKRSFIEDLLFNKVTLA) functional avidity ranged from 3.80 μg/ml to 8.33 μg/ml, with a mean of 6.54 μg/ml, roughly 5-fold lower than the functional avidity for HCoV-NL63 S peptide (Figure 4D). These data demonstrate significantly reduced functional avidity of the crossreactive SARS-CoV-2 T cell response relative to the CCC response ($P = 0.0011$; Figure 4D), compatible with an antigenic imprinting mechanism. Using genetically diverse patient-derived lymphoblastoid cell lines (LCLs), the restricting allele for these crossreactive epitopes was mapped to HLA-DPA1*01:03/HLA-DPB*04 (Supplemental Figure 8, A–C, and Supplemental Table 2). Consistent with this restriction, both HLA-DPA1*01:03/HLA-DPB*04:01 and HLA-DPA1*01:03/HLA-DPB*04:02 are predicted to bind the SARS-CoV-2 and HCoV-NL63 peptides at an IC_{50} of less than 500 nM (http://tools.iedb.org/mhcii/).

To further assess the quality of the functional T cell response, we compared the magnitude of SARS-CoV-2/CCC crossreactive T cell expansion with that of monoreactive T cell expansion in the ViraFEST assay (Figure 5A). We ordered the TCRs by descending expansion frequency in response to SARS-CoV-2 S to visualize the expansive capacity of in vitro clonotypic expansion of monoreactive clones as well as the clonotypic expansion of crossreactive TCRs in response to SARS-CoV-2 S or CCC. Crossreactive clones ($n = 51$; red) had in general less expansion in response to SARS-CoV-2 S than monoreactive clones ($n = 40$; blue), as noted by their clustering on the bottom of the chart (Figure 5A). To quantify the difference in relative fold change in response to SARS-CoV-2 S and CCC, we compared clones crossreactive for SARS-CoV-2 S and HCoV-NL63 S ($n = 46$), since HCoV-NL63 S was the only CCC tested in every ViraFEST assay. The CCP crossreactive clones had a significantly lower level of antigen-specific expansion in response to the SARS-CoV-2 S protein relative to the NL63 S protein ($P = 3.89 \times 10^{-12}$; Figure 5B). This trend was also observed when comparing the highest CCC-specific expansion (Supplemental Figure 9B). Interestingly, SARS-CoV-2 crossreactive clonotypic expansions were significantly lower than SARS-CoV-2 monoreactive expansions in CCPs ($P = 1.34 \times 10^{-6}$; Figure 5C). Together, these data demonstrate reduced expansion of CCP clones with crossreactive TCRs for SARS-CoV-2 and support our hypothesis that a subset of observed T cell responses to SARS-CoV-2 likely resulted from preexisting crossreactive clones rather than through de novo priming by SARS-CoV-2 infection.

Detection of recall SARS-CoV-2/CCC crossreactive CD4⁺ T cells in SARS-CoV-2–unexposed donors. The crossreactivity detected in CCPs could have been generated by recent infection with SARS-CoV-2 or primed by past infection with a CCC. To explore the possibility that memory CD4⁺ T cells against SARS-CoV-2 resulted from prior CCC exposure, we used the ViraFEST assay to test CD4⁺ T cells obtained from 7 healthy donors between 2017 and May 2019, before the COVID-19 pandemic (PC1–PC7; Supplemental Tables 1 and 2, and Supplemental Figure 2, A–G). SARS-CoV-2/CCC crossreactivity was detected in PC3, PC4, and PC5 (Figure 6). Notably, the CAWSVGGNYGTYF clone, identified as being SARS-CoV-2/CCC crossreactive in convalescent patients CCP4, CCP5, and CCP6, also functionally expanded in the PC3 ViraFEST assay (Figure 6A), confirming the existence of crossreactive memory CD4⁺ T cell responses at the clonal level prior to SARS-CoV-2 exposure. Interestingly, SARS-CoV-2 S–specific CD4⁺ responses without crossrecognition of a tested CCC were detected in some PC donors (Supplemental Figure 2, A, B, and E–G, and Supplemental Data), a phenomenon that has been described previously and is possibly due to reactivity against untested or undiscovered coronaviruses or other pathogens (29) or low level crossreactivity not picked up in our assay. Accordingly, the number of monoreactive clonotypes detected in PC donors ranged from 0 to 6, compared with a range of 7 to 41 in CCPs (Supplemental Data). Taken together, these data support the idea that clonal crossreactive memory CD4⁺ T cell responses existed prior to the COVID-19 pandemic and that these clonotypes maintain their antigen-specific in vitro expansive ability and can be identified by restimulation of CCC and SARS-CoV-2 S protein antigens.

SARS-CoV-2/CCC crossreactive TCRs share strong sequence homology within and among patients. It has been shown that TCRs with shared viral antigen specificity may converge toward biased distribution of variable gene usage or CDR3 sequence identity (32). This is supported by TCR Vβ CDR3 sequence homology studies and may result from immunodominant epitopes (33), HLA superfamilies (34), and/or repeated stimulation by epitopes to which there is crossrecognition (35). We therefore investigated TCR Vβ CDR3 sequence homology of the SARS-CoV-2 mono- and crossreactive TCRs identified in our study. We calculated the Levenshtein distance between all crossreactive TCRs. Seven different crossreactive TCR Vβ CDR3 sequences with high sequence homology (mutual Levenshtein distance ≤ 3) were found in 4 patients (PC3, CCP4, CCP5, and CCP6; Figure 7 and Supplemental Figure 10). Similarly, homology between SARS-CoV-2 S reactive TCR Vβ CDR3s was observed both within (CCP5) and between multiple patients (CCP1–3, -5, -7, -8, -10, PC1–2; Supplemental Figure 11). This phenomenon is not unexpected and is often seen in response to pathogens (36). Indeed, we observe TCR homology in clones reactive to the CEF pool we used as a positive control (Supplemental Figure 12). However, when combined with our data demonstrating multiple crossreactive TCRs converging to recognize a single 17 mer SARS-CoV-2 epitope, the data suggest marked TCR convergent evolution toward recognition of immunodominant epitopes in a TCR Vβ CDR3 sequence-dependent manner.

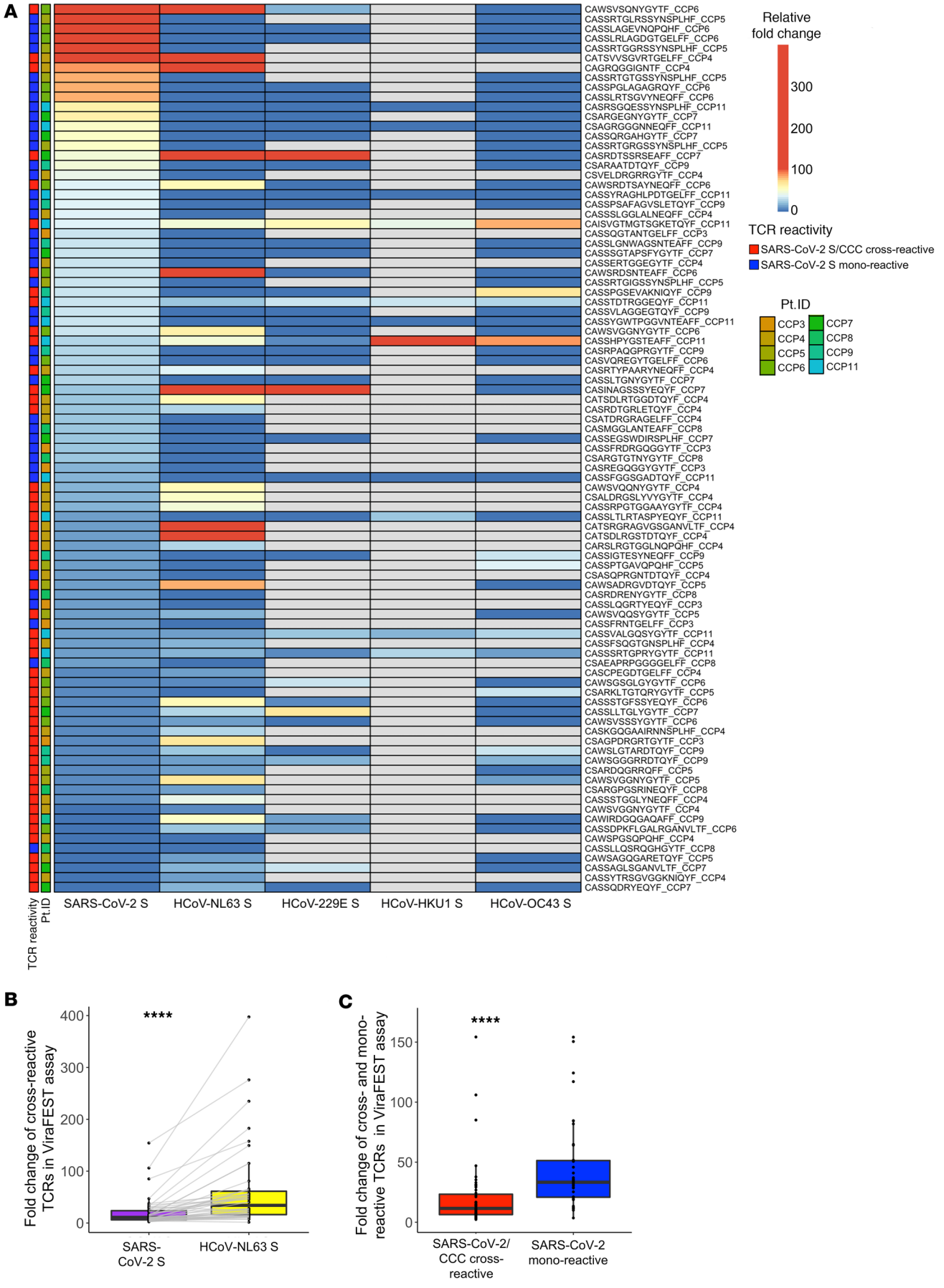
A
CAWSVSQNYGYTF_CCP6
CASSRTGLRSSYNSPLHF_CCP5
CASSLAGEVNQPQHF_CCP6
CASSLRLAGDGTGELFF_CCP6
CASSRTGGRSSYNSPLHF_CCP5
CATSVVSGVRTGELFF_CCP4
CAGRQGGIGNTF_CCP4
CASSRTGTGSSYNSPLHF_CCP5
CASSPGLAGAGRQYF_CCP6
CASSLRTSGVYNEQFF_CCP6
CASRSGQESSYNSPLHF_CCP11
CSARGEGNYGYTF_CCP7
CSAGRGGGNNEQFF_CCP11
CASSQRGAHGYTF_CCP7
CASSRTGRGSSYNSPLHF_CCP5
CASRDTSSRSEAFF_CCP7
CSARAATDTQYF_CCP9
CSVELDRGRRGYTF_CCP4
CAWSRDTSAYNEQFF_CCP6
CASSYRAGHLPDTGELFF_CCP11
CASSPSAFAGVSLETQYF_CCP9
CASSSLGGLALNEQFF_CCP4
CAISVGTMGTSGKETQYF_CCP11
CASSQGTANTGELFF_CCP3
CASSLGNWAGSNTEAFF_CCP9
CASSSGTAPSFYGYTF_CCP7
CASSERTGGEGYTF_CCP4
CAWSRDSNTEAFF_CCP6
CASSRTGIGSSYNSPLHF_CCP5
CASSPGSEVAKNIQYF_CCP9
CASSTDTRGGEQYF_CCP11
CASSVLAGGEGTQYF_CCP9
CASSYGWTPGGVNTEAFF_CCP11
CAWSVGGNYGYTF_CCP6
CASSHPYGSTEAFF_CCP11
CASRPAQGPRGYTF_CCP9
CASVQREGYTGELFF_CCP6
CASRTYPAARYNEQFF_CCP4
CASSLTGNYGYTF_CCP7
CASINAGSSSYEQYF_CCP7
CATSDLRTGGDTQYF_CCP4
CASRDTGRLETQYF_CCP4
CSATDRGRAGELFF_CCP4
CASMGGLANTEAFF_CCP8
CASSEGSWDIRSPLHF_CCP7
CASSFRDRGQGGYTF_CCP3
CSARGTGTNYGYTF_CCP8
CASREGQGGYGYTF_CCP3
CASSFGGSGADTQYF_CCP11
CAWSVQQNYGYTF_CCP4
CSALDRGSLYVYGYTF_CCP4
CASSRPGTGGAAYGYTF_CCP4
CASSLTLRTASPYEQYF_CCP11
CATSRGRAGVGSGANVLTF_CCP4
CATSDLRGSTDTQYF_CCP4
CARSLRGTGGLNQPQHF_CCP4
CASSIGTESYNEQFF_CCP9
CASSPTGAVQPQHF_CCP5
CSASQPRGNTDTQYF_CCP4
CAWSADRGVDTQYF_CCP5
CASRDRENYGYTF_CCP8
CASSLQGRTYEQYF_CCP3
CAWSVQQSYGYTF_CCP5
CASSFRNTGELFF_CCP3
CASSVALGQSYGYTF_CCP11
CASSFSQGTGNSPLHF_CCP4
CASSSRTGPRYGYTF_CCP11
CSAEAPRPGGGGELFF_CCP8
CASCPEGDTGELFF_CCP4
CAWSGSGLGYGYTF_CCP6
CSARKLTGTQRYGYTF_CCP5
CASSSTGFSSYEQYF_CCP6
CASSLLTGLYGYTF_CCP7
CAWSVSSSYGYTF_CCP6
CASKGQGAAIRNNSPLHF_CCP4
CSAGPDRGRTGYTF_CCP3
CAWSLGTARDTQYF_CCP9
CAWSGGGRRDTQYF_CCP9
CSARDQGRRQFF_CCP5
CAWSVGGNYGYTF_CCP5
CSARGPGSRINEQYF_CCP8
CASSSTGGLYNEQFF_CCP4
CAWSVGGNYGYTF_CCP4
CAWIRDGQGAQAFF_CCP9
CASSDPKFLGALRGANVLTF_CCP6
CAWSPGSQPQHF_CCP4
CASSLLQSRQGHGYTF_CCP8
CAWSAGQGARETQYF_CCP5
CASSAGLSGANVLTF_CCP7
CASSYTRSGVGGKNIQYF_CCP4
CASSQDRYEQYF_CCP7
TCR reactivity
Pt.ID
SARS-CoV-2 S
HCoV-NL63 S
HCoV-229E S
HCoV-HKU1 S
HCoV-OC43 S
Relative fold change
300
200
100
0
TCR reactivity
SARS-CoV-2 S/CCC cross-reactive
SARS-CoV-2 S mono-reactive
Pt.ID
CCP3
CCP4
CCP5
CCP6
CCP7
CCP8
CCP9
CCP11
B
Fold change of cross-reactive TCRs in ViraFEST assay
400
300
200
100
0
****
SARS-CoV-2 S
HCoV-NL63 S
C
Fold change of cross- and mono-reactive TCRs in ViraFEST assay
150
100
50
0
****
SARS-CoV-2/ CCC cross-reactive
SARS-CoV-2 mono-reactive

Figure 5. Functional activity of SARS-CoV-2 S crossreactive and monoreactive CD4⁺ T cell responses in CCP donors. A heatmap was generated to visualize the fold change of SARS-CoV-2/CCC crossreactive (red) and SARS-CoV-2 monoreactive (blue) T cell clonotypes relative to the negative control (**A**) as detected in the ViraFEST assays of CCP donors. Each row represents a single TCR Vβ CDR3 clonotype, and each column represents a peptide pool. To account for clones that were only present in 1 condition, a pseudocount of 1 was added to all clonotype counts and frequency was recalculated. Fold change was then computed by dividing frequency in response to a peptide of interest (i.e., SARS-CoV-2 S or CCC S) over the negative control (HIV). Rows were ordered by fold change of SARS-CoV-2 S in descending order. Red represents high relative fold change, and blue represents low relative fold change. The average fold change was calculated to compare overall functional avidity of crossreactive clones for SARS-CoV-2 S relative to HCoV-NL63 S for each clonotype (n = 46; **B**), and to compare relative functional activity for the SARS-CoV-2 pool between crossreactive (n = 51) and monoreactive clones (n = 40; **C**). Each dot represents a SARS-CoV-2 S–reactive clonotype from a sample, with gray line indicating a pair. Wilcoxon's signed-rank test was performed to compare the fold change of crossreactive clones in response to HCoV-NL63 S vs. SARS-CoV-2 S. Mann-Whitney U test was used to compare the fold change of SARS-CoV-2 S monoreactive vs. crossreactive clones. ****$P \leq 0.0001$.

Discussion

Most individuals infected with SARS-CoV-2 recover quickly and without long-term complications. Unfortunately, COVID-19 leads to ARDS, chronic health complications, and death in other patients. The immunologic correlates of distinct clinical outcomes remain incompletely defined. CD4⁺ T cells are requisite effectors of antiviral immunity and critical to formation of high-affinity neutralizing antibodies, shown to prevent SARS-CoV-2 infection and limit viral spread (37). Not surprisingly, SARS-CoV-2–specific CD4⁺ T cell responses are detected in most COVID-19 patients and studies have estimated that a substantial proportion of SARS-CoV-2–unexposed individuals have memory T cell responses against SARS-CoV-2. This reactivity has been shown to be the result of crossreactivity for one or more CCCs that are responsible for mild and sometimes asymptomatic upper respiratory illnesses (16–18). However, whether this is true crossreactivity mediated by one or several T cell clonotypes has not been explored. In addition, whether specific crossreactive clones expand less efficiently in response to SARS-CoV-2 is unknown. We studied the clonal nature of crossreactive CD4⁺ T cell responses to SARS-CoV-2 using the ViraFEST assay. This assay uniquely identifies antigen-specific TCR Vβ clonotypes and enables concurrent evaluation for T cell crossreactivity at the clonal level. Additionally, this is the first report, to our knowledge, using the ViraFEST assay to query CD4⁺ T cell responses. Our data show that CD4⁺ T cells that crossrecognize CCC and SARS-CoV-2 S peptides existed as memory T cell clones prior to the COVID-19 pandemic.

Bacher et al. recently studied the functional avidity of SARS-CoV-2/CCC crossreactive T cell response in unexposed individuals and COVID-19 patients (29). Our findings presented here align with the primary conclusion of this study that crossreactive T cells exhibit lower avidity relative to monoreactive T cells. However, in contrast to this study, we were able to detect crossreactive responses in COVID-19 patients, likely the result of using the T cell proliferation readout of the ViraFEST assay compared with activation marker upregulation. Nonetheless, we present here what we believe is the first report of the identity and avidity of crossreactive TCR clonotypes and their prevalence. These findings suggest some of the SARS-CoV-2–specific CD4⁺ T cell responses detected in COVID 19 patients may be the result of preexisting crossreactivity rather than de novo priming by SARS-CoV-2 infection. Although we are limited by the number of patients and number of TCRs tested, the patterns of functional avidity and support by other recent literature provide strength for our claim (13, 16, 17, 29, 31). It is worth noting that of only 12 COVID-19 convalescent patients in whom ViraFEST assays were performed, 8 patients possessed crossreactive T cell responses and 3 patients had shared TCRs, thus making it likely that SARS-CoV-2/CCC crossreactive responses are common and that these are mediated by public TCR clonotypes. It is notable that in 4 unrelated donors (3 CCPs and 1 unexposed donor), identical TCRs contributed to their endogenous SARS-CoV-2/CCC crossreactive memory CD4⁺ T cell response. Similarly, TCR cloning was based on single-cell TCR sequencing of a single subject's T cells; however, the cloned TCRs corresponded to memory CD4⁺ T cells detected in 4 different donors (CCP4, CCP5, CCP6, and PC3), reflecting a shared SARS-CoV-2–specific memory T cell repertoire. While these patients all share a common restricting allele — specifically HLA DPA1*01:03 and DPB1*04 was shared among CCP4, CCP5, CCP6, and PC3 (Supplemental Table 2) — it could also be the result of HLA/epitope degeneracy such that one or several immunodominant epitopes bind to multiple related MHC class II alleles. The epitope recognized by these TCRs is located in a conserved motif that is present in CCCs and in avian coronaviruses (22) and is targeted by crossreactive antibodies (31). CCP4 has several different CD4⁺ T cell clonotypes recognizing this same conserved immunodominant epitope. Thus, this epitope may represent a target for a universal coronavirus vaccine. It is intriguing that the crossreactive TCRs in our study targeted this region, whereas the mapped monoreactive responses targeted epitopes in the less conserved N-terminal domain. This may represent true biology, i.e., more conserved regions are more likely to induce crossreactive responses, or could be an observation limited to the TCRs that were mapped for epitope specificity in our study.

It is possible that SARS-CoV-2 infection in a subset of patients leads to preferential expansion of preexisting crossreactive memory T cells that were generated in response to prior CCC infections. Our data suggest these crossreactive T cells have lower functional avidity TCRs for SARS-CoV-2 and do not proliferate to the same degree as monoreactive SARS-CoV-2–specific CD4⁺ T cells. These findings strongly suggest a mechanism of antigenic imprinting (sometimes termed original antigenic sin), in which naive high-affinity T cell clones are outcompeted by lower affinity crossreactive memory T cell clones in individuals previously infected with a viral strain expressing the crossreactive epitope. This has been demonstrated for other viral infections (38, 39), but not for SARS-CoV-2. Accordingly, SARS-CoV-2 "monoreactive" responses were detected in cells obtained prior to the COVID-19 pandemic, possibly due to missed crossreactive responses to unknown CCCs or other pathogens (29). A limitation of the present study is the lack of matched pre-COVID and COVID biospecimens from the same donor, which may have enabled us to further understand the source of pre-COVID SARS-CoV-2–specific responses. In contrast to the

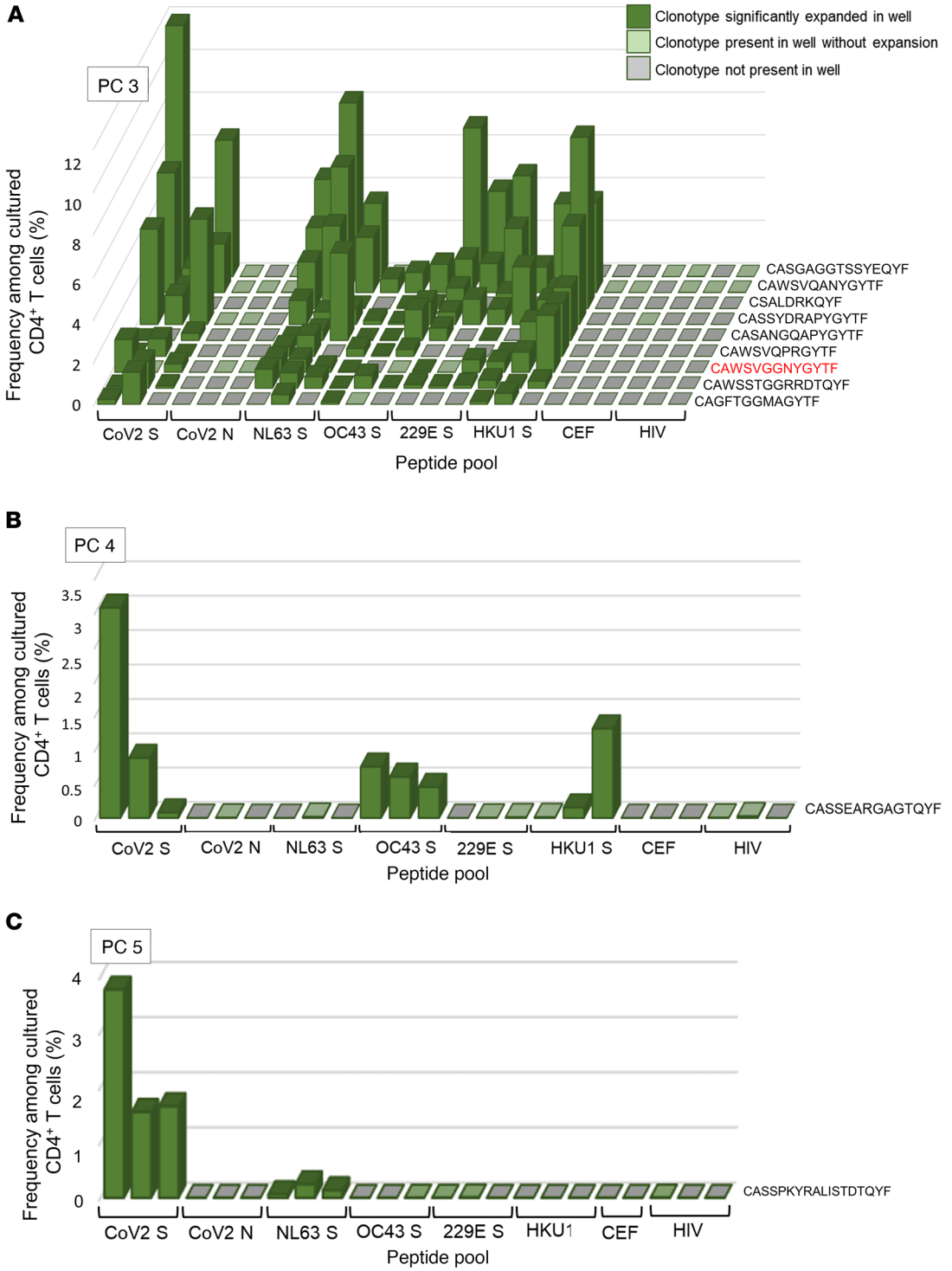

Figure 6. Detection of recall SARS-CoV-2/CCC crossreactive CD4⁺ T cells in unexposed donors. The ViraFEST assay was used to probe peripheral blood CD4⁺ T cells obtained prior to the COVID-19 pandemic (2011–2018) for reactivity to SARS-CoV-2 S and N as well as CCCs (HCoV-NL63, HCoV-OC43, HCoV-229E, and HCoV-HKU1) as cell number allowed. The assay was performed in triplicate unless otherwise noted. Responses were detected in PC3 (**A**), PC4 (**B**), and PC5 (**C**). Data are shown as the frequency (%) after culture (*y* axis) of antigen-specific CD4⁺ T cell clonotypes (*z* axis) for all peptide pools tested (*x* axis). Solid green bars represent significant (FDR < 0.05) clonotypic expansion in response to the indicated antigenic peptide pool(s), whereas translucent green color indicates the clonotype was present at low frequency in the well but did not significantly expand. Gray indicates the relevant TCR clonotype was not detected in that well. An identical, shared TCR Vβ CDR3 amino acid clonotype corresponding to crossreactive memory CD4⁺ T cells, previously identified in CCP4, CCP5, and CCP6, is shown in red.

antigenic-imprinting hypothesis, the crossreactive responses could alternatively lead to an earlier adaptive immune response to SARS-CoV-2, resulting in earlier control of viral replication, as has been described with some crossreactive vaccine-induced influenza-specific T cell responses (39, 40).

A limitation of our approach is that we focused on the S protein, whereas other studies have characterized crossreactive T cells that recognize other viral proteins (17, 18). However, to our knowledge, this is the first time crossreactive TCRs that recognize SARS-CoV-2 and CCC antigens have been identified and characterized at the clonal level. While crossreactive T cells have been shown to influence disease outcomes (41), more systematic analyses should be performed to determine how best to modulate this response to improve clinical outcome or treatment/vaccine efficacy. Taken together, our data have major implications for coronavirus vaccine design and could potentially partially explain heterogeneous clinical outcomes in COVID-19 patients.

Methods

Study participants, biospecimens, and HLA haplotyping. The term CCPs refers to patients who tested positive for SARS-CoV-2 by nasal-swab PCR test, were symptomatic but not hospitalized, and have since recovered from COVID-19. The term PCs refers to peripheral blood mononuclear cell (PBMC) donors whose blood was drawn and processed prior to the SARS-CoV-2 epidemic (between 2017 and May 2019) (42). The median age of the 12 CCPs was 38.5 years (range 21 to 72 years). There were 8 males and 4 females. Two of the subjects were Hispanic. There were 8 White, 2 African American, 1 Asian, and 1 multiracial individual. All of the subjects except CCP2 had mild disease and were not hospitalized. CCP2 had well-controlled HIV on antiretroviral therapy and developed severe disease. Leukapheresis product was commercially purchased for all unexposed donors between 2011 and 2018 (STEMCELL Technologies). PBMCs from each study participant and unexposed donor were isolated from leukapheresis product or whole blood via Ficoll-Paque PLUS (Cytiva) gradient centrifugation and were viably cryopreserved at –140°C or were used immediately in FEST assay. CCP4 LCLs were conducted via EBV transformation of peripheral blood B cells at the Genetic Resources Core Facility, Johns Hopkins Institute of Genetic Medicine. Low-resolution MHC class I and II haplotyping was performed on DNA from each subject at the Johns Hopkins Hospital Immunogenetics Laboratory. High resolution was used for CCP4, CCP5, CCP6, PC3, PC5, PC6, PC7, and all additional LCLs at the Johns Hopkins Hospital Immunogenetics Laboratory.

Identification of human coronavirus-specific T cells. Overlapping peptide pools spanning the S protein of 4 common human coronaviruses (HCoV-NL63, HCoV-OC43, and HCoV-229E, BEI and JPT; and HCoV-HKU1, JPT), as well as overlapping peptide pools spanning the S and N proteins of SARS-CoV-2 (BEI and JPT) were used to stimulate $CD4^+$ T cells in the ViraFEST assay as described previously (23), with minor modifications. Briefly, 2×10^6 PBMCs were plated in culture medium (IMDM, 5% human AB serum, 10 IU/ml IL-2, 50 μg/mL gentamicin) with 10 μg/ml of individual HCoV and CoV-2 peptide pools, a positive control CEFX Ultra SuperStim consisting of pooled CEF MHC II–restricted epitopes (PM-CEFX-3, JPT), a negative control HIV-1 Nef peptide pool (NIH AIDS Reagents), or without peptide. Each assay condition was performed in triplicate unless otherwise noted. On day 3, half the media was replaced with fresh culture media containing IL-2 (final concentration of 10 IU/mL IL-2). On day 7, half the media was replaced with fresh culture media containing IL-2 (final concentration of 10 IU/ml IL-2). On day 10, cells were harvested and $CD4^+$ T cells were isolated using the EasySep $CD4^+$ T cell isolation kit (STEMCELL, 17952). DNA was extracted from cultured $CD4^+$ T cells using the QIAmp Micro-DNA Kit according to the manufacturer's instructions (QIAGEN). TCR-Seq of DNA extracted from cultured $CD4^+$ T cells was performed by the Johns Hopkins FEST and TCR Immunogenomics Core Facility (FTIC) using the Oncomine TCR Beta Short-Read Assay (Illumina Inc). Samples were pooled and sequenced on an Illumina iSeq 100 using unique dual indexes.

Data preprocessing was performed to eliminate nonproductive TCR sequences and to align and trim the nucleotide sequences to obtain only the CDR3 region. Sequences not beginning with C or ending with F or W and having fewer than 7 amino acids in the CDR3 were eliminated. Resultant processed data files were uploaded to our publicly available MANAFEST analysis web app (http://www.stat-apps.onc.jhmi.edu/FEST/) to bioinformatically identify antigen-specific T cell clonotypes. Clones were considered positive based on the following criteria: (a) significantly expanded in the culture of interest (in 2 of 3 replicate wells) compared with the reference culture (PBMCs cultured with 10 IU/ml IL-2 and HIV-1 Nef pool or media without peptide for HIV^+ donor CCP2) at an FDR less than the specified threshold (<0.05; default value), (b) significantly expanded in the culture wells of interest compared with every other culture well performed in tandem (FDR < 0.05; default value), and (c) having an odds ratio greater than 5 (default value). To identify crossreactive responses, we used statistical criteria established previously (26, 29).

Detection of antigen-specific T cell clonotypes in naive and memory $CD4^+$ T cells. Naive and memory $CD4^+$ T cells were isolated from cryopreserved PBMCs by first isolating $CD4^+$ T cells from bulk PBMCs using the EasySep Human $CD4^+$ T cell Enrichment Kit (STEMCELL, 19052) followed by using the EasySep Human Naive $CD4^+$ T cell Enrichment Kit (STEMCELL, 19555). DNA was extracted from $CD4^+$ T cells using the QIAmp Micro-DNA Kit according to the manufacturer's instructions. Deep TCR sequencing of DNA extracted from $CD4^+$ T cells was performed by the Johns Hopkins FEST and TCR Immunogenomics Core Facility (FTIC) using the Adaptive Biotechnologies immunoSEQ human TCR-β kit.

Separately, 10^5 naive or memory $CD4^+$ T cells isolated using the methods above were plated separately at a 1:1 ratio with T cell–depleted PBMCs and cultured with a CEF peptide pool (5 μg/ml). The ViraFEST culture was performed as described above. After 10 days of culture, all cells were harvested, and DNA was extracted from cultured cells using the QIAmp Micro-DNA Kit according to the manufacturer's instructions. Survey TCR-Seq of DNA extracted from cultured $CD4^+$ T cells was performed by the Johns Hopkins FEST and TCR Immunogenomics Core Facility (FTIC) using the Adaptive Biotechnologies immunoSEQ human TCR-β kit. Data preprocessing was performed, and all data were uploaded to our publicly available MANAFEST analysis web app (http://www.stat-apps.onc.jhmi.edu/FEST/) to bioinformatically identify antigen-specific T cell clonotypes. The same statistical criteria mentioned above were used to determine CEF-specific T cell clonotypes. All SARS-CoV-2 S and CEF-reactive TCR Vβ CDR3 sequences identified in previous ViraFEST assays were searched for in the TCR-Seq TSV data files from cultured and uncultured naive and memory $CD4^+$ T cells. The frequency

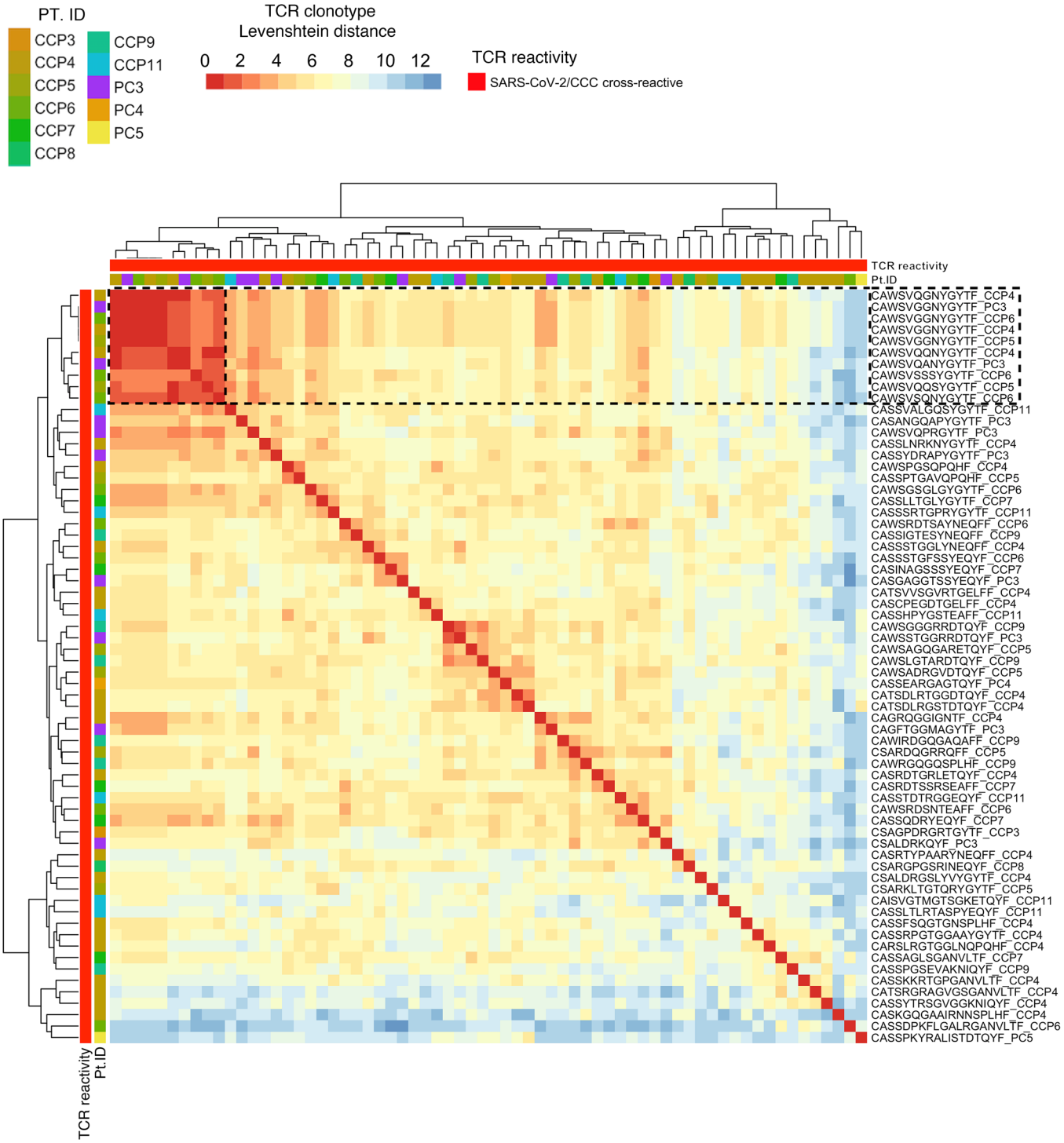

Figure 7. Shared sequence homology of SARS-CoV-2/CCC crossreactive TCRs within and among patients. A heatmap was generated to visualize sequence homology of crossreactive clones within and between the patients in our study. Each row/column represents a crossreactive clonotype in a sample. Colors represent the levels of sequence homology using Levenshtein distance, with red indicating high degree of sequence homology and blue less sequence similarity. Different colors were used to distinguish patient samples in the color sidebar. The black box highlights an area of high sequence homology across multiple patients with Levenshtein distance of 3 or less.

of clones present in at least 1 naive or memory population was plotted using GraphPad Prism (version 9.0.2).

Intracellular staining of T cell activation cytokines. 10^7 PBMCs from CCP6 and CCP12 were cultured in R10 media with 10 IU/ml IL-2 and 5 μg/ml SARS-CoV-2 S or HCoV-NL63 S or without peptide for 10 to 12 days. At the end of the culture period, cells were washed and plated in fresh R10 media with 10 IU/ml IL-2 and rested overnight prior to restimulation with 5 μg/ml SARS-CoV-2 S or HCoV-NL63 S or without peptide. Protein transport inhibitors (GolgiPlug, 1 μg/ml; GolgiStop, 0.7 μg/ml) as well as antibodies against CD28 and CD49d (BD

Biosciences) were added to the cultures. Following a 12-hour stimulation, the cells were washed and stained with annexin V (BV-421, BD Biosciences, 563973), CD3 (APC-Cy7, BioLegend, 300426), and CD4 (PerCP-Cy-5.5, BioLegend, 300530). We then fixed, permeabilized, and stained the cells intracellularly for cytokines IFN-γ (APC, BD Biosciences, 506510) and IL-2 (PE, BioLegend, 500307). Flow cytometry was done on a BD FACS LSR Fortessa flow cytometer, and data were analyzed with FlowJo, version 10. A minimum of 100,000 lymphocytes were collected and analyzed.

Identification of the cognate TCR-α for SARS-CoV-2– and HCoV-CCC–specific Vβ CDR3s. PBMCs from CCP4 were cultured for 10 days with SARS-CoV-2 S, SARS-CoV-2 N, and HCoV-NL63 S peptide pools as described above. On day 10, live $CD4^+$ T cells were FACS sorted and subjected to single cell 5′ VDJ sequencing to identify phased TCR-α and TCR-β chain sequences at single-cell resolution using the 10x Genomics Chromium Single Cell 5′ VDJ sequencing platform on a chromium controller (10x Genomics) to achieve a target cell capture rate of 10,000 individual cells per sample. All samples were processed simultaneously, and the resulting libraries were prepared in a single batch following the manufacturer's instructions for VDJ library preparation. The resulting 5′ VDJ libraries were subjected to next-generation sequencing at the Sidney Kimmel Comprehensive Cancer Center Experimental and Computational Genomics Core. Resulting data were preprocessed and analyzed using cellranger VDJ software (10x Genomics) and visualized using Loupe V(D)J browser (10x Genomics) to identify the paired TCR Vα chain for the cognate CDR3 Vβ chains identified by ViraFEST. IMGT Repertoire was used to identify the full amino acid sequence for each V and J gene for both the TCR-α and TCR-β chains.

Generation of a Jurkat reporter cell line. A gBlock was created with the human constant regions and the full TCR-α and TCR-β chains separately (Integrated DNA Technologies [IDT]). To generate a Jurkat reporter cell in which we could transfer our TCRs of interest, the endogenous TCR-α and TCR-β chains were knocked out of a specific Jurkat line that contains a luciferase reporter driven by an NFAT-response element (Promega) using the Alt-R CRISPR system (IDT). Two sequential rounds of CRISPR knockout were performed using crDNA targeting the TCR-α constant region (AGAGTCTCTCAGCTGGTACA) and the TCR-β constant region (AGAAGGTGGCCGAGACCCTC). crDNA and tracrRNA (IDT) were resuspended at 100 μM with Nuclear-Free Duplex Buffer (IDT). They were duplexed at a 1:1 molar ratio according to the manufacturer's instructions. The duplexed RNA was cooled to room temperature before mixing with Cas9 Nuclease at a 1.2:1 molar ratio for 15 minutes, and 40 pmols of Cas9 RNP complexed with gRNA were mixed with 500,000 cells in 20 μl of OptiMEM, loaded into a 0.1 cm cuvette (Bio-Rad), and electroporated at 90 V and 15 ms using an ECM 2001 (BTX). Cells were transferred to complete growth medium and expanded for 7 days. Limiting dilution was used to acquire single cell clones, and gDNA was harvested using the Quick-DNA 96 Kit (Zymo Research). The regions flanking the CRISPR cut sites were PCR amplified (TCR-α forward primer: GCCTAAGTTGGGGAGACCAC; reverse primer: GAAGCAAGGAAACAGCCTGC; TCR-β forward primer: TCGCTGTGTTTGAGCCATCAGA, reverse primer: ATGAACCACAGGTGCCCAATTC) and Sanger sequenced. Only TCR-α^-/β^- clones were selected. Complete knockout was confirmed by failure to restore CD3 expression on electroporation with only a TCR-α or TCR-β chain, and successful CD3 expression on electroporation with both TCR chains.

CD8 was transduced into the TCR-α^-/β^- Jurkat reporter cells using the MSCV Retroviral Expression System (Clontech). gBlocks (IDT) encoding CD8α and CD8β chains separated by a T2A self-cleaving peptide were cloned into the pMSCVpuro retroviral vector by HiFi DNA assembly (New England Biolabs). The plasmid was then cotransfected with a pVSV-G envelope vector into the GP2-293 packaging cell line per the manufacturer's instructions. Viral supernatant was harvested 48 hours after transfection and concentrated 20-fold using Retro-X Concentrator (Clontech). For transduction, non–tissue culture–treated 48-well plates were coated with 150 μL retronectin (Clontech) in PBS at 10 μg/mL overnight at 4°C. Plates were then blocked with 10% FBS for 1 hour at room temperature, followed by washing once with PBS. After removing PBS, viral particles and 2×10^5 of TCR-α^-/β^- Jurkat reporter cells were added to each well in a total volume of 500 μL cell culture media. Plates were spun at 2000*g* for 1 hour at 20°C, then incubated at 37°C. Selection with 1 μg/mL puromycin (Thermo Fisher Scientific) began 3 days later. Single-cell clones were established by limiting dilution, and clones were subsequently screened for CD8 expression by flow cytometry. To generate a Jurkat reporter line that expresses both CD4 and CD8, CD4 viral particles were produced and transduced into the CD8-expressing Jurkat reporter cells using similar procedures.

Jurkat TCR transfer. TCRs of interest were introduced into the CD4/CD8 TCR-α^-/β^- Jurkat reporter line by cloning the TCR-α and TCR-β chains separately into the pCI vector (Promega) by HiFi DNA assembly (New England Biolabs). The 2 plasmids were coelectroporated into the TCR-α^-/β^- Jurkat reporter line using 4 mm cuvettes (Bio-Rad) and 275V for 10 ms for 3 pulses at a 0.1 interval between pulses. Cells were rested in RPMI 10% FBS at 37°C for 24 hours. TCR expression efficiency was assessed by CD3 expression using flow cytometry. After rest, live Jurkat cells were counted and plated at a 1:1 ratio with patient-matched LCLs and peptide pools. Peptide titrations were carried out from 50 μg/ml to 1.25 μg/ml to assess TCR reactivity to peptide pools. Cells and peptides were cocultured for 24 hours. TCR activity was assessed by NFAT-luciferase reporter readout using the Bio-Glo Luciferase Assay System (Promega).

Epitope identification and avidity analysis. Crossreactive and monoreactive TCRs were cloned into the Jurkat reporter cell line and plated at a 1:1 ratio with patient-derived LCLs. They were first tested for reactivity to minipools consisting of 10 peptides making up the entirety of the SARS-CoV-2 or HCoV-NL63 S protein. Once the reactive minipool was identified, the same TCRs were again transfected into Jurkats and plated with LCLs and the individual SARS-CoV-2 and HCoV-NL63 peptides representing the stimulating minipool. Once the specific peptide was identified, we did peptide titrations from 20 μg/ml to 0.15 μg/ml to assess TCR avidity for each stimulating peptide. TCR activity was again assessed by NFAT-luciferase reporter readout using Bio-Glo Luciferase Assay System (Promega). TCR EC_{50} was calculated by identifying the peptide concentration (μg/ml) required to reach one-half plateaued RLU. If 20 μg/ml of peptide was insufficient to maximize Jurkat-TCR activation, then we estimated EC_{50} by calculating the peptide concentration (μg/ml) required to read one-half maximum RLU reached in our assay. TCR EC_{50} was then used as a metric to estimate TCR relative avidity for individual 17 mer peptides. Two-tailed Student's *t* test was performed using the mean of the EC_{50}

of crossreactive TCRs for SARS-CoV-2 and the mean of the EC_{50} of monoreactive TCRs for SARS-CoV-2.

Heatmaps and unrooted phylogenetic trees. The nonredundant TCR sequences were defined by excluding the first 3 and last 3 amino acids of the TCR Vβ CDR3 region due to significant sequence overlap at the beginning and end of the CDR3 sequence (36, 43). The Levenshtein distance between each pair of TCR sequences was calculated based on nonredundant TCRs, using the stringdist R package (44). The TCR sequence homology pattern was visualized in a heatmap and an unrooted phylogenetic tree, where each row of the heatmap and each leaf of the unrooted phylogenetic tree represented a TCR Vβ CDR3 sequence from a sample. The heatmap and unrooted phylogenetic tree were generated using the pheatmap and ape R packages respectively. All analyses were performed using R software, version 3.6.1.

Statistics. Wilcoxon's signed-rank test was performed to compare the fold change of crossreactive clones in response to NL63 S versus SARS-CoV-2 S and CCC S versus SARS-CoV-2 S. Mann-Whitney *U* test was used to compare the fold change of SARS-CoV-2 S monoreactive versus crossreactive clones. $P < 0.05$ was considered statistically significant.

Study approval. This study was conducted according to Declaration of Helsinki principles and was approved by the IRB of Johns Hopkins University. All study participants gave written, informed consent before their inclusion in this study.

Data availability. All raw TCR sequencing data have been made publicly available. Illumina data were deposited in the NCBI's Sequence Read Archive (SRA BioProject PRJNA 705196, $CD4^+$ T Cell Receptor Sequencing of COVID-19 Convalescent, Vaccinated, or Pre-COVID Healthy Donors). PC5-7 and additional naive versus memory experiments were sequenced using the Adaptive Biotechnologies TCR-sequencing kit, and those data can be accessed from the Adaptive Biotechnologies ImmuneACCESS Repository (DOI: 10.21417/AGBZ2021JCI, https://clients.adaptivebiotech.com/admin/pub/dykema-2021-jci).

Author contributions

AGD, BAW, CCG, LSC, DC, SB, RR, JXC, EHCH, KC, EAT, AKK, DS, and ST performed experiments and acquired data. BZ, LA, JZ, SY, SZ, and HJ led the bioinformatic and computational analyses. AAO, AP, FRD, JDP, DMP, ALC, KNS, and JNB led study design and data interpretation. All authors contributed to experimental planning, data analysis and interpretation, and manuscript preparation.

Acknowledgments

Funding for this work was provided by The Bloomberg~Kimmel Institute for Cancer Immunotherapy, The Johns Hopkins University Provost, The Immune-Viral Landscape in COVID-19 Pneumonia-ARDS: IVAR study, The Bill and Melinda Gates Foundation (134582), NIH Cancer Center Support grant P30 CA006973, and NIH grants R37CA251447, U19A1088791, P41EB028239, R01AI153349, R01AI145435-A1, R21AI149760, and U54CA260492. We would like to thank Bert Vogelstein and Kenneth W. Kinzler for helpful discussions and assistance with TCR cloning, Paul F. Robbins and Rami Yossef for help with TCR cloning, Jennifer Myers, Anuj Gupta, and the Experimental and Computational Genomics Core at the Sidney Kimmel Comprehensive Cancer Center for support with next-generation sequencing and preprocessing of 10x Genomics single cell 5′ VDJ data, the Sidney Kimmel Comprehensive Cancer Center FEST and TCR Immunogenomics Core Facility (FTIC) for support with ViraFEST assays and TCR sequencing, and Adaptive Biotechnologies for helpful discussions. Graphical abstract and study-time line images were created with BioRender.com. We thank our respective clinical, laboratory, and administrative teams as well as the patients and their families. The specimens utilized for this publication were part of the Johns Hopkins Biospecimen Repository, which relies on the contribution of many patients, research teams, and clinicians.

Address correspondence to: Kellie N. Smith, Bloomberg~Kimmel Institute for Cancer Immunotherapy, Johns Hopkins University, Baltimore, Maryland 21218, USA. Phone: 410.502.7523; Email: kellie@jhmi.edu. Or to: Joel N. Blankson, Department of Medicine, School of Medicine, Johns Hopkins University, Baltimore, Maryland 21218, USA. Phone: 410.502.9920; Email: jblanks@jhmi.edu.

1. Huang C, et al. Clinical features of patients infected with 2019 novel coronavirus in Wuhan, China. *Lancet*. 2020;395(10223):497–506.
2. Richardson S, et al. Presenting characteristics, comorbidities, and outcomes among 5700 patients hospitalized with COVID-19 in the New York City area. *JAMA*. 2020;323(20):2052–2059.
3. van de Ven K, et al. Systemic and respiratory T-cells induced by seasonal H1N1 influenza protect against pandemic H2N2 in ferrets. *Commun Biol*. 2020;3(1):564.
4. Sridhar S, et al. Cellular immune correlates of protection against symptomatic pandemic influenza. *Nat Med*. 2013;19(10):1305–1312.
5. Todryk SM, et al. Correlation of memory T cell responses against TRAP with protection from clinical malaria, and $CD4^+$ CD25 high T cells with susceptibility in Kenyans. *PLoS One*. 2008;3(4):e2027.
6. Walsh EE, et al. Clinical impact of human coronaviruses 229E and OC43 infection in diverse adult populations. *J Infect Dis*. 2013;208(10):1634–1642.
7. Sagar M, et al. Recent endemic coronavirus infection is associated with less-severe COVID-19. *J Clin Invest*. 2021;131(1): e143380.
8. Killerby ME, et al. Human coronavirus circulation in the United States 2014-2017. *J Clin Virol*. 2018;101:52–56.
9. Edridge AWD, et al. Seasonal coronavirus protective immunity is short-lasting. *Nat Med*. 2020;26(11):1691–1693.
10. Galanti M, Shaman J. Direct observation of repeated infections with endemic coronaviruses. *J Infect Dis*. 2021;223(3):409–415.
11. Le Bert N, et al. SARS-CoV-2–specific T cell immunity in cases of COVID-19 and SARS, and uninfected controls. *Nature*. 2020;584(7821):457–462.
12. Grifoni A, et al. Targets of T cell responses to SARS-CoV-2 coronavirus in humans with COVID-19 disease and unexposed individuals. *Cell*. 2020;181(7):1489–1501.
13. Sekine T, et al. Robust T cell immunity in convalescent individuals with asymptomatic or mild COVID-19. *Cell*. 2020;183(1):158–168.
14. Braun J, et al. SARS-CoV-2–reactive T cells in healthy donors and patients with COVID-19. *Nature*. 2020;587(7833):270–274.
15. Ng KW, et al. Pre-existing and de novo humoral immunity to SARS-CoV-2 in humans. *Science*. 2020;370(6522):1339–1343.
16. Woldemeskel BA, et al. Healthy donor T-cell responses to common cold coronaviruses and SARS-CoV-2. *J Clin Invest*. 2020;130(12):6631–6638.
17. Mateus J, et al. Selective and cross-reactive SARS-CoV-2 T cell epitopes in unexposed humans. *Science*. 2020;370(6512):89–94.
18. Nelde A, et al. SARS-CoV-2–derived peptides

define heterologous and COVID-19-induced T cell recognition. *Nat Immunol*. 2021;22(1):74–85.
19. Weiskopf D, et al. Phenotype and kinetics of SARS-CoV-2–specific T cells in COVID-19 patients with acute respiratory distress syndrome. *Sci Immunol*. 2020;5(48):eabd2071.
20. Meckiff BJ, et al. Single-cell transcriptomic analysis of SARS-CoV-2 reactive CD4$^+$ T cells [preprint]. https://doi.org/10.1101/2020.06.12.148916. Posted on bioRxiv July 13, 2020.
21. Petrova G, et al. Cross-reactivity of T cells and its role in the immune system. *Crit Rev Immunol*. 2012;32(4):349–372.
22. Robson B. COVID-19 Coronavirus spike protein analysis for synthetic vaccines, a peptidomimetic antagonist, and therapeutic drugs, and analysis of a proposed achilles' heel conserved region to minimize probability of escape mutations and drug resistance. *Comput Biol Med*. 2020;121:103749.
23. Danilova L, et al. The Mutation-Associated Neoantigen Functional Expansion of Specific T cells (MANAFEST) assay: a sensitive platform for monitoring antitumor immunity. *Cancer Immunol Res*. 2018;6(8):888–889.
24. Forde PM, et al. Neoadjuvant PD-1 blockade in resectable lung cancer. *N Engl J Med*. 2018;378(21):1976–1986.
25. Smith KN, et al. Persistent mutant oncogene specific T cells in two patients benefitting from anti-PD-1. *J Immunother Cancer*. 2019;7(1):40.
26. Chan HY, et al. A T cell receptor sequencing-based assay identifies cross-reactive recall CD8+ T cell clonotypes against autologous HIV-1 epitope variants. *Front Immunol*. 2020;11:1–9.
27. Anagnostou V, et al. Evolution of neoantigen landscape during immune checkpoint blockade in non-small cell lung cancer. *Cancer Discov*. 2017;7(3):264–276.
28. Le DT, et al. Mismatch repair deficiency predicts response of solid tumors to PD-1 blockade. *Science*. 2017;357(6349):409–413.
29. Bacher P, et al. Low-avidity CD4(+) T cell responses to SARS-CoV-2 in unexposed individuals and humans with severe COVID-19. *Immunity*. 2020;53(6):1258–1271.
30. Wintjens R, et al. Impact of glycan cloud on the B-cell epitope prediction of SARS-CoV-2 Spike protein. *NPJ Vaccines*. 2020;5:81.
31. Morgenlander WR, et al. Antibody responses to endemic coronaviruses modulate COVID- 19 convalescent plasma functionality. *J Clin Invest*. 2021;137(7):e146927.
32. Gil A, et al. Epstein-Barr virus epitope-major histocompatibility complex interaction combined with convergent recombination drives selection of diverse T cell receptor α and β repertoires. *mBio*. 2020;11(2):e00250–20.
33. Kedzierska K, et al. Conserved T cell receptor usage in primary and recall responses to an immunodominant influenza virus nucleoprotein epitope. *Proc Natl Acad Sci U S A*. 2004;101(14):4942–4947.
34. Shen WJ, et al. The utility of supertype clustering in prediction for class II MHC-peptide binding. *Molecules*. 2018;23(11):1–18.
35. Li H, et al. Determinants of public T cell r esponses. *Cell Res*. 2012;22(1):33–42.
36. Glanville J, et al. Identifying specificity groups in the T cell receptor repertoire. *Nature*. 2017;547(7661):94–98.
37. Chandrashekar A, et al. SARS-CoV-2 infection protects against rechallenge in rhesus macaques. *Science*. 2020;369(6505):812–817.
38. Mongkolsapaya J, et al. T cell responses in dengue hemorrhagic fever: are cross-reactive T cells suboptimal?. *J Immunol*. 2006;176(6):3821–3829.
39. Nelson SA, Sant AJ. Imprinting and editing of the human CD4 T cell response to influenza virus. *Front Immunol*. 2019;10:932.
40. Nienen M, et al. The role of pre-existing cross-reactive central memory CD4 T-cells in vaccination with previously unseen influenza strains. *Front Immunol*. 2019;10:593.
41. Saletti G, et al. Older adults lack SARS CoV-2 cross-reactive T lymphocytes directed to human coronaviruses OC43 and NL63. *Sci Rep*. 2020;10(1):21447.
42. Cox AL, et al. Prospective evaluation of community-acquired acute-phase hepatitis C virus infection. *Clin Infect Dis*. 2005;40(7):951–958.
43. Hou X, et al. Analysis of the repertoire features of TCR beta chain CDR3 in human by high-throughput sequencing. *Cell Physiol Biochem*. 2016;39(2):651–667.
44. van der Loo MPJ. The stringdist package for approximate string matching. *R. J*. 2014;6(1):111–122.